Journal of Power Sources 271 (2014) 431–436

Contents lists available at ScienceDirect

Journal of Power Sources

journal homepage: www.elsevier.com/locate/jpowsour

Surface-layer formation by reductive decomposition of $LiPF_6$ at relatively high potentials on negative electrodes in lithium ion batteries and its suppression

Tomoya Kawaguchi [a, *], Koki Shimada [a], Tetsu Ichitsubo [a], Shunsuke Yagi [b], Eiichiro Matsubara [a]

[a] Department of Materials Science and Engineering, Kyoto University, Kyoto 606-8501, Japan
[b] Nanoscience and Nanotechnology Research Center, Osaka Prefecture University, Osaka 599-8570, Japan

HIGHLIGHTS

- Surface layer on negative electrodes was investigated for $LiPF_6$/EC–DMC electrolyte.
- In-situ X-ray reflectivity analyses etc revealed a surface layer (other than SEI).
- The layer was formed by a reductive decomposition of $LiPF_6$ around 2.6 V vs Li.
- Such an inactive surface layer influences the battery performance.
- How to circumvent the formation of the passivate layer was discussed.

ARTICLE INFO

Article history:
Received 15 April 2014
Received in revised form
26 July 2014
Accepted 2 August 2014
Available online 15 August 2014

Keywords:
Lithium ion batteries
Negative electrode
Reductive decomposition
Electrolyte
$LiPF_6$

ABSTRACT

In using a $LiPF_6$/ethylene carbonate–dimethyl carbonate electrolyte for lithium ion batteries (LIBs), a certain reductive reaction is known to occur at a relatively high potential (ca. 2.6 V vs. Li^+/Li) on Sn electrode, but its details are still unknown. By means of in-situ X-ray reflectometry, X-ray photoelectron spectroscopy, scanning electron microscopy observations and electrochemical measurements (by using mainly Sn electrode, and additionally Pt, graphite electrodes), we have found out that this reduction eventually forms an inactive passivation-layer consisting mainly of insulative LiF ascribed to the reductive decomposition of $LiPF_6$, which significantly affects the battery cyclability. In contrast, a solid-electrolyte interphase (SEI) is formed by the reductive reaction of the solvent at ca. 1.5 V vs. Li^+/Li, which is lower than the reduction potential of $LiPF_6$. However, we have found that the formation of SEI preempts that of the passivation layer when holding the electrode at a potential lower than 1.5 V vs. Li^+/Li. Consequently, the cyclability is improved by suppressing the formation of the inactive passivation layer. Such a pretreatment would be quite effective on improvement of the battery cyclability, especially for a relatively noble electrode whose oxidation potential is between 1.5 V and 2.6 V vs. Li^+/Li.

1. Introduction

The surface layer, formed on a negative electrode by the reductive decomposition of an electrolyte in Li ion batteries (LIBs), passivates the electrode surface and prevents a further decomposition of the electrolyte on the surface. The surface layer having a good Li ion conductivity in addition to a sufficient electrical isolation [1,2] is often called “solid-electrolyte interphase (SEI)”. The properties of the surface layer dominate the various battery performances, e.g. the irreversible capacity, power and the degradation of the battery. Although there have been many works on those formed by the reduction reaction of the solvent [3–6], few studies have been reported on the influences on battery properties of a surface layer formed due to the decomposition of a solute. However, through an atomic force microscope observation, Lucas et al. [7] reported a certain small change on a surface of a Sn negative electrode at ca. 2.6 V vs. Li^+/Li during cyclic voltammetry (CV) scan. It is expected that the surface morphologic change at the high potential can be ascribed to the reductive decomposition of the solute, because the potential of 2.6 V is higher than the reduction

* Corresponding author.
E-mail address: kawaguchi.tomoya.55a@st.kyoto-u.ac.jp (T. Kawaguchi).

http://dx.doi.org/10.1016/j.jpowsour.2014.08.010
0378-7753/

potential of the solvent, ca. 1.5 V vs. Li^+/Li, at which the SEI is formed by the reductive reaction of the EC–DEC/DMC solvent (EC: ethylene carbonate, DEC: diethyl carbonate, DMC: dimethyl carbonate). However, the details of the reductive reaction at the relatively high potential has not been understood yet to date.

It is thus worthwhile to investigate a mechanism and influences on the battery properties of the reductive reaction around 2.6 V vs Li^+/Li. In the present work, by using a two-electrode cell composed of a Sn electrode, a Li electrode, and a $LiPF_6$/EC–DMC electrolyte, we have found out that a considerably thick surface layer formed due to the reduction reaction at about/below 2.6 V in a two-electrode-CV profile. As demonstrated in the pioneering works, [8–10] the in-situ X-ray reflectivity (XRR) measurement is a quite suitable for analyzing characteristics of thin surface layers. Then, in combination with the in-situ XRR measurement, scanning electron microscopy (SEM), X-ray photoelectron spectroscopy (XPS), and conventional electrochemical measurements, here we have evaluated the properties (such as density, thickness, composition, etc.) of the surface layers formed on the electrode. Based on the results, we discuss a plausible formation mechanism of the surface layer on the electrode. In addition, $LiClO_4$ was also tested as a solute instead of $LiPF_6$ to check whether or not the surface layer is formed without F ion species in the electrolyte. Furthermore, we have examined whether the similar surface layer is formed on Pt and graphite electrodes, instead of Sn. Finally, we mention the degradation behaviors in battery cycle tests by comparing two kinds of electrodes with the different surface layers formed by holding the electrodes at 2.0 V and 1.2 V, being higher and lower than the SEI formation voltage.

2. Experimental

2.1. Electrode preparation and battery construction

Flat and smooth Sn electrode samples for in-situ XRR measurements were prepared on a Si wafer by DC-magnetron sputtering at room temperature. For the XRR analyses, the sputtering time and the power were set at 300 s and 50 W, respectively. For the battery tests, a relatively thick Sn electrodes were prepared on Cu foils by sputtering for 900 s with 50 W. Pt plates mechanically polished with an emery paper were used for electrodes, and pyrolytic graphite plates (Panasonic) were used for graphite electrodes.

A two-electrode-cell consisting of the above electrodes as a “positive” electrode, a lithium metal sheet (Honjo Metal) as a “negative” electrode and an electrolyte with 1 M $LiPF_6$ or 1 M $LiClO_4$ (EC/DMC = 1/2 in volume, Kishida Chemical) were sealed in a laminated aluminum cell in an Ar-gas-filled glove box, where both moisture and oxygen content were less than 2 ppm. Water contents in the electrolytes were measured to be less than 80 ppm by Karl Fischer titrations (KEM, MKC-610). A cell/applied voltage set for the two-electrode-cell is, of course, not exactly equal to the value based on a Li reference electrode. However, since the current densities used in the present electrochemical measurements were small, so that the polarization of Li electrode is considered to be negligibly small, and we use the cell voltage in a unit of “V (vs. Li)”.

2.2. Electrochemical tests and in-situ XRR measurement

A cyclic voltammetry (CV) test and a battery cycle test were performed by a potentiostat/galvanostat (Biologic, VMP3), where the positive electrode was defined as a working electrode (WE) and the Li negative electrode was a counter/reference electrode (CE/RE); the two-electrode-CV scan was carried out from the initial OCV to 0.01 V at a sweep rate of 0.1 mV s^{-1}. In the battery charge/discharge cycle test, the current was set at a rate of 1C (0.07 mA cm^{-2}) for the Sn electrode, and the cut off voltages were set at 1.2 V and 0.01 V for charge and discharge, respectively. The Sn electrodes for the battery tests were prepared by holding them at 2.0 and 1.2 V for 5 h before the tests to compare the effects of the surface layers formed at these two potentials on the battery cyclability.

Parallel and monochromatic Mo Kα radiation was obtained for XRR measurements by using the rotating anode X-ray generator, RINT-2500 (RIGAKU), with a Ge(111) single crystal incident monochromator. In-situ XRR profiles for the working electrode were obtained by decreasing the cell voltage from the initial open circuit voltage (OCV = 2.80 V) with a potentiostat/galvanostat (Biologic, SP200); to obtain each XRR profile, the positive electrode was kept for 30 min at each voltage, where each step was 25 mV, corresponding to the average scan rate of 0.014 mV s^{-1}.

2.3. SEM observation and XPS analyses

Images of surface and cross section of the electrodes were observed by a field-emission scanning electron microscopy (JEOL JSM-6500F). For the FE-SEM observation, two kinds of discharged (lithiated) Sn electrodes were prepared by holding the electrodes at 2.55 V and 1.2 V for 12 h in the $LiPF_6$ electrolyte, respectively. The electrode samples were taken out from the cell, washed by the solvent (EC/DMC = 1/2 in v/v) and then by DMC in the glove box, dried for 1 h in vacuum, and transported to the SEM in an Ar gas atmosphere.

Chemical bondings of the surface layer formed on the Sn electrode were investigated by X-ray photoemission spectroscopy (XPS, JEOL JPS-9010TRX) with Mg Kα radiation (1254 eV), and those of the bulk (or near the Sn bulk) were also evaluated from the profiles after etching by Ar-ion sputtering at 300 eV. The electrode samples for the XPS analyses were prepared in the same procedure as those for the SEM observations; the typical samples were prepared by holding at 2.0 V and 1.2 V for 12 h in the same electrolyte. The energy calibration was done with Si 2p (99.7 eV) coming from the Si wafer.

3. Results

Fig. 1 shows the CV profile obtained for the Sn electrode. The profiles below 0.77 V show the typical CV for the formation of Sn–Li compounds. [3,11,12] In the higher voltage region, three cathodic peaks are observed at 1.40, 1.70, and 2.55 V in the first cycle. The peaks at 1.40 and 1.70 V (“b”, surrounded by a solid line square) are

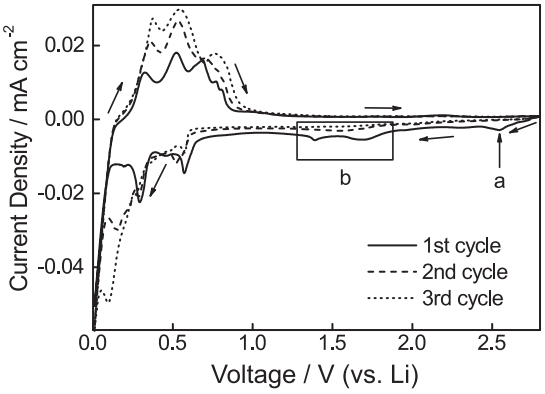

Fig. 1. Cyclic voltammogram of the Sn electrode between 0.01 and 2.80 V at a sweep rate of 0.1 mV s^{-1} in a mixed EC/DMC solvent with 1 M $LiPF_6$ solute. Arrows indicate the direction of the sweep.

ascribed to the formation of a surface layer (so-called SEI) due to the reduction reaction of the solvent [6,13,14]. As before, in the present study, we focus the surface layer formed at about 2.55 V ("a" in Fig. 1).

Fig. 2 compares the potential dependences of the charge amount by the reduction reaction on the Sn electrodes in the electrolyte with $LiPF_6$ (open circle) and $LiClO_4$ (black triangle). The cathodic peak at about 2.6 V was clearly observed in using the $LiPF_6$ electrolyte, while the peak around 2.6 V was not observed in the $LiClO_4$ electrolyte. Incidentally, the charge amount estimated for decomposition of the impurity water (less than 80 ppm) in the $LiPF_6$ electrolyte cannot explain the observed reduction charge amount around 2.6 V in Fig. 2. Thus, it is considered that the reduction reaction at 2.6 V originates from the solute $LiPF_6$.

Fig. 3(a) and (b) shows the in-situ XRR profiles of the Sn electrodes in the EC–DMC electrolyte with $LiPF_6$ and $LiClO_4$ at the voltages indicated by alphabets in Fig. 2, respectively. The XRR profiles at 0.145°, which corresponds to the critical angle θ_c of metal Sn in the electrolyte, remains virtually unchanged from "a" to "d" in Fig. 3(a). A drastic shift of the critical angle to a lower angle is observed in the voltage between "d" (2.6 V) and "e" (2.575 V), which indicates that a certain rough surface layer of low density was formed on the Sn electrode. In contrast, as found from Fig. 3(b), such a drastic profile change cannot be observed even when swept down to 2.0 V in using the $LiClO_4$ electrolyte. Thus, it can be concluded that the surface layer formed at 2.6 V is strongly related with the solute $LiPF_6$, namely, due to the reductive decomposition of the $LiPF_6$ solute. Fig. 3(c) and (d) shows the cross sections of (c) the as-sputtered electrode and (d) the electrodes taken out from the cell after being discharged from the initial OCV to 2.55 V. By comparing two micrographs, it is obvious that a rough surface layer about 200 nm thick is formed on the surface of the Sn electrode after swept down to 2.55 V.

As before, we can observe the other cathodic peaks around 1.5 V in the CV profile ("b" in Fig. 1), which is believed to be an SEI formation. Here, to distinguish the two kinds of surface layers, we have performed XPS measurements for the two samples prepared by holding the electrodes at 2.0 V (>1.5 V) and 1.2 V (<1.5 V) in the $LiPF_6$ electrolyte. Fig. 4 shows the chemical composition along the depth direction of the two surface layers formed at those voltages. As shown in Fig. 4(a) and (b), the elements Li, F, Sn, C, O and P were detected from both the samples. It is obvious that the thickness of the surface layer formed at 1.2 V is much thinner than that formed

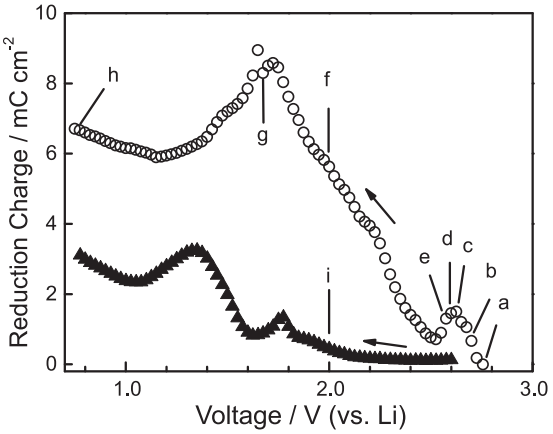

Fig. 2. The voltage dependence of the reduction charge amount on the Sn electrode in the electrolyte with 1 M $LiPF_6$ (open circle) and 1 M $LiClO_4$ (black triangle). Arrows indicate the direction of the sweep. The alphabets indicate the voltages for X-ray reflectivity (XRR) measurements, and the positive electrode was kept for 30 min at each voltage step of 25 mV.

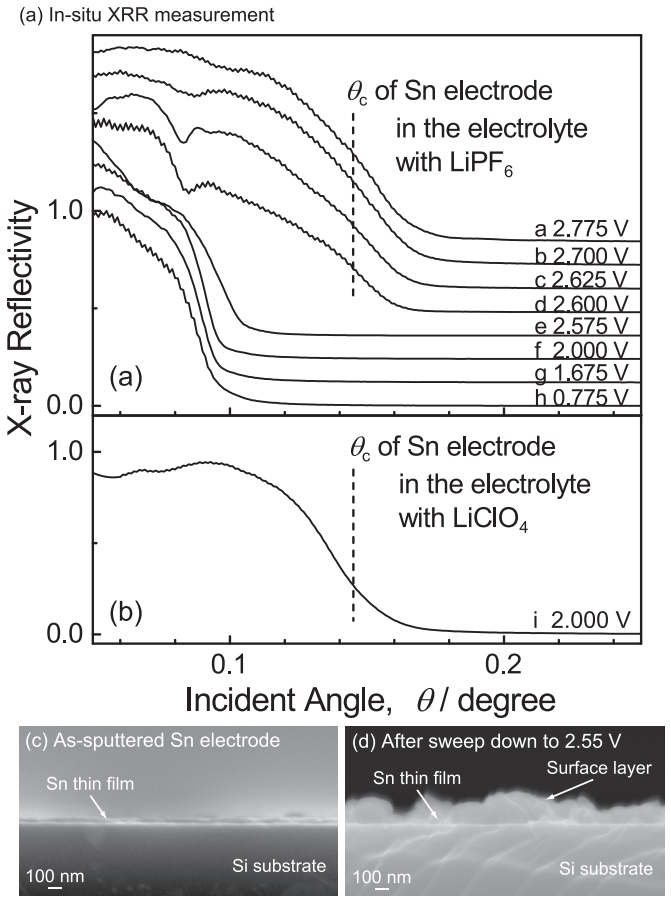

Fig. 3. (a) In-situ XRR profiles of the Sn electrode in the $LiPF_6$ electrolyte at the various voltages indicated by the alphabets in Fig. 2. (b) An XRR profile of the Sn electrode in the $LiClO_4$ electrolyte at 2.0 V. Cross sections of (c) the as-sputtered Sn electrode and (d) the Sn electrode after swept from the open circuit voltage (2.80 V) down to 2.55 V.

at 2.0 V. In the sample at 2.0 V, the signals from F, Li, and Sn are relatively strong, while C, O and P were week and immediately vanished by Ar etching. On the other, in the sample at 1.2 V, since the signals from C and O were rather dominant even after the Ar etching for the duration longer than 10 min, this layer consists mainly of some organic material related to the solvent.

Fig. 4(c) and (d) focuses the F–Li and F–Sn bondings for non-etched and Ar-etched surfaces; hereafter we refer to the former as "just surface" and the latter as "near bulk". In both samples prepared at 2.0 V and 1.2 V, while the XPS signal related with Sn–F is vanished completely near bulk (after the Ar etching for 5 min), the signal indicating Li–F remains with the Sn metal. We have clarified that the peak of the F 1s spectra near bulk is attributed to the LiF compound, [15,16] and the higher binding-energy peak of the Sn 3d spectra is attributed to the SnF_4 compound. [17,18] Thus, the surface layer formed at 2.0 V consists mainly of LiF and small amount of SnF_4 at just surface. In addition, as mentioned above, the surface layer formed at 1.2 V is much thinner than that at 2.0 V, because the relatively strong signal from the Sn metal can be observed other than SnF_4 even at just surface.

Here, as a supplementary experiment to check the universality of the reductive decomposition regardless of the kinds of electrodes, Pt and graphite electrodes were held at an appropriate voltage between 1.5 V and 2.6 V (here 2.0 V) for 12 h in the $LiPF_6$ electrolyte for the SEM observations. Fig. 5 shows the SEM images of the Pt and graphite electrodes, after it was kept for 12 h at 2.0 V. By comparing Fig. 5(a) and (b), it is found that the Pt electrode was

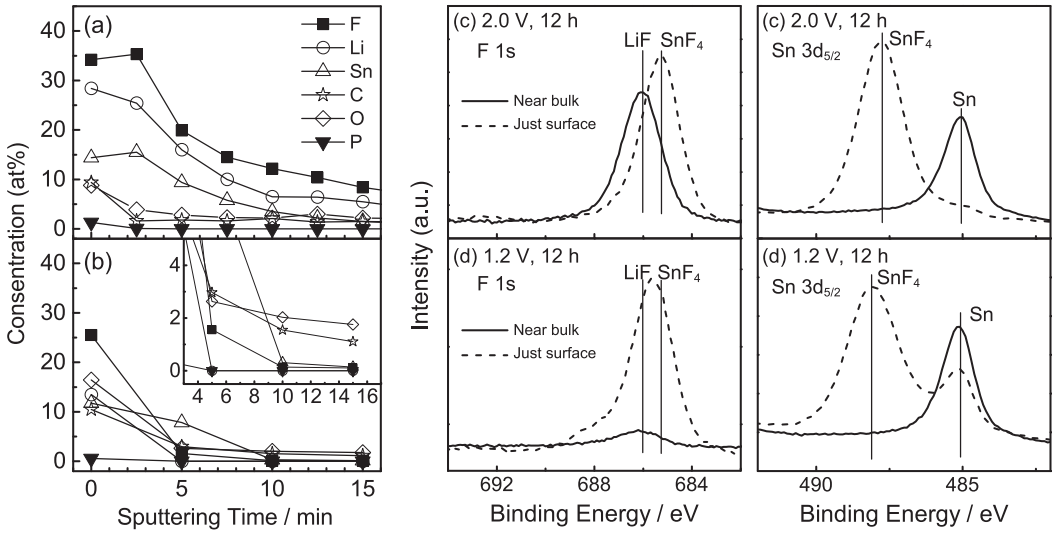

Fig. 4. XPS analyses for the two kinds of surface layers prepared by holding at 2.0 and 1.2 V for 12 h in the $LiPF_6$ electrolyte. The left figures show the depth dependence of the chemical composition for the samples at (a) 2.0 V and (b) 1.2 V (with an inset showing the magnified profile), respectively, and right figures show the F 1s (left) and Sn 3d (right) XPS spectra of (c) 2.0 V and (d) 1.2 V. In (c) and (d), the XPS spectra of the "near bulk" was obtained after Ar-etching of the as-prepared surface (i.e., "just surface" sample) at 300 eV for 5 min.

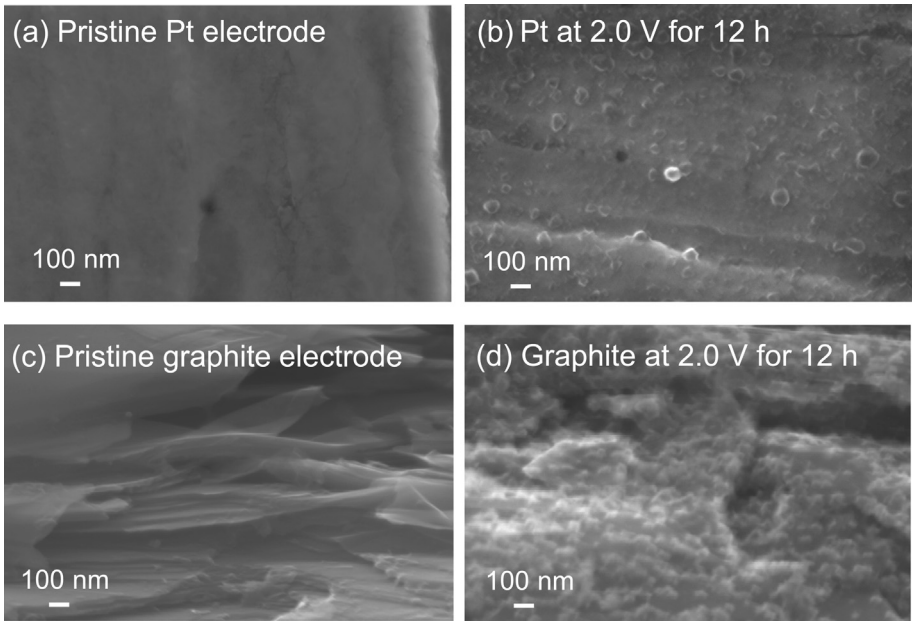

Fig. 5. SEM images of (a) pristine Pt electrode, (b) the Pt electrode held at 2.0 V for 12 h in a 1 M $LiPF_6$/EC–DMC electrolyte, (c) pristine pyrolytic graphite electrode, and (d) the pyrolytic graphite electrode held at the same condition.

covered with a thick surface layer. Similarly, as seen in Fig. 5(c) and (d), a drastic change of the surface morphology is also observed on the graphite electrode. Especially in Pt electrode, we have also conducted the electrochemical quartz microbalance (EQCM) measurement by using a three-electrode cell (WE: Pt, CE, Li, RE: Li). Fig. 6(a) and (b) shows the EQCM profile and SEM microstructure. As found from Fig. 6(a), the mass change was drastically changed around 2.6 V with a large cathodic current. In addition, as shown in Fig. 6(b), the electrode was covered with the thick surface layer; by the EDX analysis, the film composition was measured to be F: 93.4 at%, P: 1.6 at%, Pt: 4.7 at%, which indicates that the Pt electrode is substantially covered by the surface layer. Since the chemical composition of P is very small compared to that of F, the surface layer was not composed of PF_6^- or PF_3, and mainly composed of LiF (Li cannot be detected by the EDX analysis). Thus, it has been demonstrated that the formation of such a surface layer at the high potentials was observed even in Pt and also graphite electrode, and maybe universal irrespective of the kinds of electrodes.

Finally, to examine the influences of the surface layers on battery performances, we have carried out the battery cycle tests by using two kinds of the Sn electrodes prepared at 1.2 V and 2.0 V for 5 h in the $LiPF_6$ electrolyte. The difference of the battery capacities of the Sn electrodes is shown in Fig. 7. Obviously, the electrode held at 2.0 V is promptly degraded because of the presence of the surface layer consisting mainly of LiF, while the electrode kept at 1.2 V shows a relatively good cyclability. This difference is maybe due to

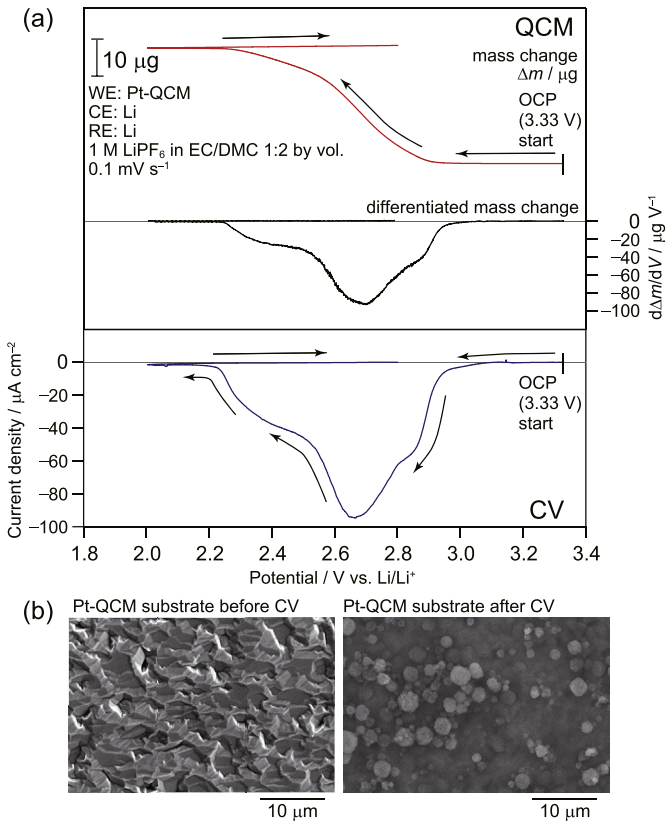

Fig. 6. (a) Mass change of Pt working electrode and cyclic voltammogram measured by EQCM during the potential sweep from open circuit potential (3.33 V vs. Li/Li^+) at 0.1 mV s^{-1} in 1 M $LiPF_6$ EC–DMC (1:2 by vol.). Differentiated mass change by potential is also shown. (b) SEM images of Pt-EQCM electrode before and after cyclic voltammetry.

the polarization difference (namely, polarization becomes large in the case of the electrode prepared at 2.0 V), which influences the charge/discharge amount till the cut-off voltage in cycling process.

4. Discussion

By in-situ XRR technique, we have found that the long-time holding of the electrode in the $LiPF_6$/EC–DMC electrolyte between 1.5 and 2.6 V eventually leads to the formation of a thick inactive passivation-layer on the electrode surface. This behavior is considerably universal without regard to the kinds of electrodes. Namely,

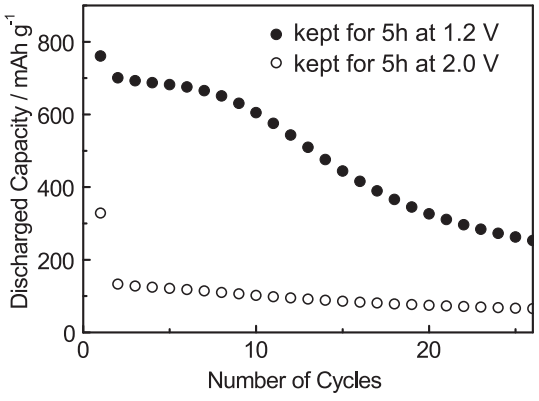

Fig. 7. Cycle tests at the rate of 1C (0.07 mA cm^{-2}) for the Sn electrodes, which were held at 2.0 and 1.2 V for 5 h in a 1 M $LiPF_6$/EC–DMC electrolyte in advance.

the surface layer formed by holding at 2.0 V was also observed on Pt and graphite electrodes as well as on the Sn electrode.

Taking account of the high chemical durability of the EC/DMC solvent at 2.55 V vs. Li^+/Li [13] and the absence of the surface-layer with the use of $LiClO_4$ instead of $LiPF_6$, the surface layer consisting mainly of LiF is considered to originate from the reductive decomposition of the $LiPF_6$ solute. According to literature, [15] a plausible main reductive reaction of the solute is considered to be.

$$PF_6^- + 2e^- + 3Li^+ \rightarrow PF_3 + 3LiF.$$

Namely, when $LiPF_6$ is reduced to be PF_3, the F^- ions are released and instantly the LiF compound can be formed on the electrode surface with Li ions in the electrolyte. Thus, the fact that the LiF formation occurs at the relatively high potential around 2.0–2.5 V can be understood as a consequence of the reductive reaction of the PF_6^- anion.

Besides the main reaction, we have to mention the formation mechanism of the SnF_4 compound. Basically, SnF_4 would be formed by a chemical reaction with hydrogen fluoride HF. It is reported that $LiPF_6$ is decomposed, with moisture impurity in the electrolyte, to $LiPF_6 + H_2O \rightarrow LiF + 2HF + PF_3O$, where the product HF reacts with the Sn electrode to form the SnF_4 compound [19,20]. An unavoidable small amount of the water always exists in the electrolyte (actual content of moisture was about 80 ppm in this study) even though we carefully treat battery components in an Ar-filled dried globe box (dew point less than −82 °C). Under the existence of H_2O, $LiPF_6$ decomposes to give various chemical components, which would result in the formation of SEI-like deposits. Hence, it is necessary to take the above reaction into consideration here. However, it should be noted that the above reaction is not an electrochemical reaction governed by the electrode potential, so that this reaction may not be involved with the thick surface-layer formed at such a high potential of 2.6 V. Actually, the SnF_4 compound was observed on “just surface” and not observed “near bulk”. Thus, the electrochemical inactive surface layer would be due to the reductive reaction at the relatively high potential.

Then, we encounter a problem of how to suppress the surface-layer formation due to the reduction of $LiPF_6$. When the electrode is held below 1.5 V (e.g., at 1.2 V in the present experiment), not only the reductive reaction of the solvent for the formation of the SEI layer, but also that of the $LiPF_6$ can occur *in principle* electrochemically. However, as shown in the SEM and XPS observations above, the surface layer formed at 1.2 V is much thinner than that formed at 2.0 V, and its composition is very different from the layer formed at 2.0 V. As a consequence, we have obtained a significant fact that the reductive reaction of the EC-DMC solvent preempts that of the $LiPF_6$ solute below 1.5 V. Although the surface layer consisting mainly of insulative LiF (and also SnF_4) seriously affects the battery performance, the electrode can circumvent the formation of the inactive passivation-layer by holding at 1.2 V prior to the battery test, by which the cyclability of the Sn electrode is significantly improved. Thus, such a pretreatment would be quite effective on the suppression of the inactive surface-layer formation and improvement of the battery cyclability.

5. Conclusions

We have investigated the formation of the inactive surface layer formed at a relatively high potential in the commonly used LIB systems. In the present experiment, the cathodic peak observed around 2.6 V is found to form the inactive surface layer consisting mainly of LiF, being due to the reductive decomposition of the $LiPF_6$ solute, which affects battery performances. Although the reduction potential is much higher than the well-known potential of 1.5 V for

the SEI formation, it has been demonstrated that the SEI formation precedes the inactive surface-layer formation that originates from the reductive decomposition of $LiPF_6$. This is a very important result for development of the LIB negative electrode, since the battery cyclability is significantly improved by the low-potential-holding pretreatment, as demonstrated in the present study. Thus, in order to obtain an excellent battery cyclability, it is recommended to be held at an appropriate potential below 1.5 V vs. Li^+/Li to form the SEI layer on a negative electrode.

Acknowledgments

The XPS analyses were technically supported by Y. Sonobayashi in Department of Materials Science and Engineering in Kyoto University. This work was partly supported by X-ray Free Electron Laser Priority Strategy Program (MEXT) of Japan Science and Technology Agency (JST). One of the authors, T. K., was greatly supported by JSPS Grant-in-Aid for JSPS Fellows numbers 25-2242.

References

[1] E. Peled, J. Electrochem. Soc. 126 (1979) 2047.
[2] E. Peled, C. Menachem, D. Bar-Tow, A. Melman, J. Electrochem. Soc. 143 (1996) L4.
[3] J.-T. Li, S.-R. Chen, X.-Y. Fan, L. Huang, S.-G. Sun, Langmuir 23 (2007) 13174.
[4] M. Inaba, T. Uno, A. Tasaka, J. Power Sources 146 (2005) 473.
[5] J.-S. Bridela, S. Grugeona, S. Laruellea, P. Jusef Hassounb, B.S. Realeb, J.-M. Tarascon, J. Power Sources 195 (2010) 2036.
[6] L.Y. Beaulieu, S.D. Beattie, T.D. Hatchard, J.R. Dahn, J. Electrochem. Soc. 150 (2003) A419.
[7] I.T. Lucas, E. Pollak, R. Kostecki, Electrochem. Commun. 11 (2009) 2157.
[8] L.G. Parrat, Phys. Rev. 95 (1954).
[9] M. Hirayama, N. Sonoyama, M. Ito, M. Minoura, D. Mori, A. Yamada, K. Tamura, J. Mizuki, R. Kanno, J. Electrochem. Soc. 154 (2007) A1065.
[10] P. Croce, G. Devant, M. Sere, M. Verhaeghe, Surf. Sci. 22 (1970) 173.
[11] K. Hirai, T. Ichitsubo, T. Uda, A. Miyazaki, S. Yagi, E. Matsubara, Acta Mater. 56 (2008) 1539.
[12] T. Ichitsubo, S. Yukitani, K. Hirai, S. Yagi, T. Uda, E. Matsubara, J. Mater. Chem. 21 (2011) 2701.
[13] K. Xu, Chem. Rev. 104 (2004) 4303.
[14] X. Zhang, R. Kostecki, T.J. Richardson, J.K. Pugh, P.N. Ross, J. Electrochem. Soc. 148 (2001) A1341.
[15] D. Aurbach, B. Markovsky, A. Shechter, Y. Ein-Eli, H. Cohen, J. Electrochem. Soc. 143 (1996) 3809.
[16] A.M. Andersson, K. Edström, J. Electrochem. Soc. 148 (2001) A1100.
[17] D. Shuttleworth, J. Phys. Chem. 84 (1980) 1629.
[18] P. Grutsch, M. Zeller, T. Fehlner, Inorg. Chem. 12 (1973) 1431.
[19] C. Nanjundiah, J.L. Goldman, L.A. Dominey, V.R. Koch, J. Electrochem. Soc. 135 (1988) 2914.
[20] S.-W. Song, S.-W. Baek, Electrochim. Acta 54 (2009) 1312.